


ORIGINAL RESEARCH

Unravelling ecophysiological and molecular adjustments in the photosynthesis-respiration balance during *Fusarium graminearum* infection in wheat spikes

Florian Rocher¹ | Pierre Bancal² | Alain Fortineau² | Géraldine Philippe¹ |
Philippe Label³ | Thierry Langin¹ | Ludovic Bonhomme¹ 

¹Université Clermont Auvergne, INRAE, UMR 1095 Génétique Diversité Ecophysiologie des Céréales, Clermont-Ferrand, France

²Université Paris-Saclay, INRAE, AgroParisTech, UMR EcoSys, Palaiseau, France

³Université Clermont Auvergne, INRAE, UMR 547 PIAF, Physique et Physiologie Intégratives de l'Arbre en environnement Fluctuant, Aubière Cedex, France

Correspondence

Ludovic Bonhomme,
Email: ludovic.bonhomme@inrae.fr

Funding information

Agence Nationale de la Recherche,
Grant/Award Numbers: 16-IDEX-0001 CAP 20-25, ANR-15-CE21-0010, CAP2025 Academy; Région Auvergne-Rhône-Alpes; European Regional Development Fund

Edited by U. Mathesius

Abstract

Wheat responses to *F. graminearum* result in a deep and sharp reprogramming of a wide range of biological processes, including energy-associated functions and related metabolisms. Although these impacts have been thoroughly described at the molecular scale through proteomics and transcriptomics studies, phenotypic studies are still needed to fill the gap between the observed molecular events and the actual impacts of the disease on the ecophysiological processes. Taking advantage of the gas exchange method, the effects of two *F. graminearum* strains of contrasting aggressiveness on spike's photosynthesis and respiration-associated processes during an early infection time course were deeply characterized. Besides, an RNAseq-based expression profiling of the genes involved in the photosynthesis, respiration and stomatal movement processes was also performed when plants were challenged using the same two fungal strains. In response to Fusarium head blight, CO₂ assimilation and CO₂ diffusion adjustments matched transcriptomic data, showing altered photosynthetic processes and sharp gene regulations unrelated to symptom development. In contrast, although ecophysiological characterization clearly demonstrated respiration adjustments along with the *F. graminearum*'s infection process, the gene regulations involved were not fully captured transcriptionally. We demonstrated that combining gas exchange methods with transcriptomics is especially effective in enhancing and deepening our understanding of complex physiological adjustments, providing unique and complementary insights that cannot be predicted from a single approach.

1 | INTRODUCTION

Fusarium Head Blight (FHB), mainly caused by the Ascomycota fungus *Fusarium graminearum*, represents a major threat to wheat (Parry et al., 1995; Goswami & Kistler, 2004; McMullen et al., 2012; Dahl & Wilson, 2018). FHB has direct impacts on yield and grain quality as

well as causes serious human health concerns through the accumulation of harmful mycotoxins (e.g., deoxynivalenol, DON) (Boyacioglu & Hettiarachchy, 1995; Argyris et al., 2003; Chen et al., 2019). Existing control strategies, i.e. the combined use of fungicides, tolerant wheat genotypes and agricultural practices, are currently insufficient to control FHB epidemics (Dahl & Wilson, 2018; Xia et al., 2020). While

This is an open access article under the terms of the [Creative Commons Attribution-NonCommercial](https://creativecommons.org/licenses/by-nc/4.0/) License, which permits use, distribution and reproduction in any medium, provided the original work is properly cited and is not used for commercial purposes.

© 2025 The Author(s). *Physiologia Plantarum* published by John Wiley & Sons Ltd on behalf of Scandinavian Plant Physiology Society.

breeding for resistance remains the most efficient way of limiting damages associated with FHB outbreaks (Mesterhazy, 2020), FHB resistance trait is strictly quantitative and involves more than 625 Quantitative Trait Loci (Zheng et al., 2021) displaying relatively small effects (Bai et al., 2018; Steiner et al., 2017; Venske et al., 2019) and strong dependency to environmental conditions (Osman et al., 2015; Steiner et al., 2017). Over the past two decades, the multiple evidence of the involvement of host's genes in the pathogen's establishment (Vogel et al., 2002), the so-called susceptibility genes (S genes), have opened new opportunities to identify new key determinants of plant diseases that can have direct application in breeding for resistance (Pavan et al., 2010; van Schie & Takken, 2014; Zaidi et al., 2018; Garcia-Ruiz et al., 2021). The importance of S genes in the outcome of wheat-*F. graminearum* interaction has already been demonstrated in several studies (Ma et al., 2006; Garvin et al., 2015; Nalam et al., 2015; Gordon et al., 2016; Hu et al., 2018; G. Li et al., 2019; Z. Su et al., 2019; Brauer et al., 2020; Hales et al., 2020; Chhabra et al., 2021; P. Su et al., 2021), making the elucidation of the mechanisms underlying wheat susceptibility to FHB a promising approach to improve FHB resistance (Fabre et al., 2020; Gorash et al., 2021).

By definition, S genes are not only involved in the setup of a compatible interaction but also in a wide range of plant fundamental processes (Lapin & Van den Ackerveken, 2013; van Schie & Takken, 2014; Engelhardt et al., 2018; Garcia-Ruiz et al., 2021). Thus, beyond their identification, it is necessary to understand their role in the basal functions of the host plant. There is a growing interest in S genes in wheat-*F. graminearum* pathosystem now requires an in-depth characterization of the biological functions and physiological processes impacted throughout the infection's progression. While omics studies have resulted in large amounts of information on the processes impacted during wheat's infection by *F. graminearum* (Fabre, Vignassa, et al., 2019; Rocher et al., 2024), the very complex nature of plant's susceptibility to pathogens makes it necessary to fill the gap between the molecular information and the observed phenotype. More generally, this also raises outstanding questions about how pathogens can manipulate host energy metabolism, carbon gain and allocation, notably by interfering with chloroplastic photosynthetic processes and their interplay with mitochondrial respiration. Both chloroplast and mitochondria represent central hubs of plant physiology that interconnect a wide array of biological processes, including photosynthesis and respiration, respectively, as well as Reactive Oxygen Species (ROS) production, hormone synthesis (Jasmonate and Salicylic acid), programmed cell death signalling, calcium signalling and the synthesis of specialized metabolites. Hence, while being involved in primary metabolism functions, those two organelles are also important sensors and drivers of plant stress responses (Lee et al., 2011; Colombatti et al., 2014; Caplan et al., 2015; Huang et al., 2016; Lu & Yao, 2018; Littlejohn et al., 2021; Wang et al., 2022). Such control of basal processes makes chloroplast and mitochondria important targets in the pathogen's infection strategy through the delivery of specific molecules, the so-called effectors, in the host tissues to divert plant primary metabolism and defence

mechanisms (de Torres Zabala et al., 2015; Q. Xu et al., 2019; Kretschmer et al., 2020; G. Xu et al., 2020; Figueroa et al., 2021; Tzelepis et al., 2021). In the wheat-*F. graminearum* pathosystem, a recent proteomics study highlighted a deep remodelling of the chloroplast functions in response to FHB between 48 h and 72 h post-inoculation (Fabre, Vignassa, et al., 2019). Furthermore, three effectors, Fg03600 (Jin et al., 2024), FgTPP1 (Darino et al., 2024) and FgCWM1 (Zhang et al., 2024), hijacking plant immunity through the interaction with chloroplastic and mitochondrial-associated proteins have been validated. More generally, this also raises outstanding questions about how pathogens can manipulate host energy metabolism, carbon gain and allocation, notably by interfering with photosynthetic processes and their interplay with mitochondrial respiration.

However, so far, the phenotypic characterization of wheat-*F. graminearum* interaction is mainly limited to the monitoring of symptoms, fungal mass and DON concentration (Mesterhazy, 2020), and it does not provide any information on the impacted biological processes. Thus, breaking down the susceptibility mechanisms into their main physiological components is necessary. For this purpose, non-invasive techniques, such as gas-exchange measurements, have been successfully applied to several pathosystems (Horst et al., 2010; Carretero et al., 2011; Debona et al., 2014; Gortari et al., 2018), can provide new insights into the physiological status of wheat's spikes during the interaction with *F. graminearum*, especially with regards to photosynthesis- and respiration-related process.

This work addresses an in-depth characterization of the physiological status of wheat's spikes facing two *F. graminearum* strains of contrasting aggressiveness using gas-exchange analyses. The main objectives were to investigate the pathogen-induced perturbations in photosynthesis and respiration and to connect the obtained data with the transcriptomics profiling of wheat's FHB-responsive genes involved in those two biological processes.

2 | MATERIAL AND METHODS

2.1 | Experimental procedures for ecophysiological experiments

Two independent gas exchange experiments, referred to as ambient and saturation light experiments (Figure 1A), were conducted on the bread wheat cultivar 'Recital', an FHB-susceptible genotype. Plants used in both gas exchange experiments were grown and inoculated using the same procedure described in the following sections. The two experiments differed in terms of the light intensity applied when the measures were performed. Ambient light measurements were performed under a Photosynthetic Photon Flux Density (PPFD) of $616 \mu\text{mol m}^{-2} \text{s}^{-1}$, while the saturation light measurements were done under a PPFD of $968 \mu\text{mol m}^{-2} \text{s}^{-1}$ (Fortineau & Bancal, 2018). In the saturation light experiment, the plants were placed in a light adaptation device (Figure 1B-(1)) set up in the growth chamber 10 min prior to daytime measurements. This device, consisting of four vertical

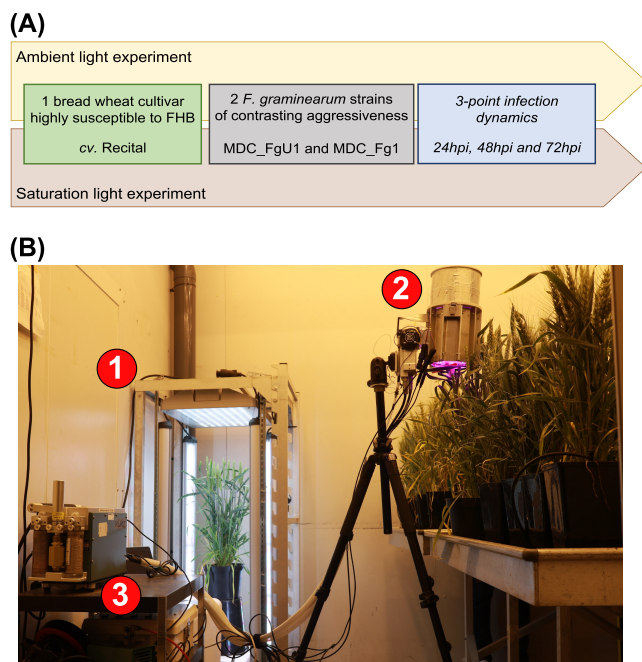


FIGURE 1 Overview of the experimental design of the study. Two independent experiments were performed with 2 light conditions, one with ambient light and the other one by adapting the plants at saturation light 10mn before the measures. For both experiments, the susceptible cultivar ‘Recital’ was inoculated with two *F. graminearum* strains, MDC_FgU1 and MDC_Fg1 in increasing order of aggressiveness, and with water for the controls. Gas exchange measures were performed at 24, 48 and 72 hpi (hpi: hours post inoculation). The photo shows (1) the device used for the light adaptation and (2) the measure chamber connected to (3) the LICOR 6400 device.

LED bars (BL120c, Valoya) and one top LED panel (GentleSpace gen², Philips Lighting France Signify), allowed to apply a total PPFD of $1400 \mu\text{mol m}^{-2} \text{s}^{-1}$.

2.1.1 | Plant production and growth conditions

For both experiments, wheat plants were sown in buckets, vernalized at 4°C and, transplanted in 4 L pots and grown in the same controlled growth chamber with an automatic watering system, as previously described in Rocher et al. (2022). After three weeks of tillering at 12/12 h light cycle and 17/15°C (day/night), the plants were grown under the following conditions: 16/8 h light cycle and 21/17°C (day/-night) temperatures. The relative humidity in the growth chamber remained constant and set at 80%. At spike height, the measured PPFD is $520 \mu\text{mol m}^{-2} \text{s}^{-1}$.

2.1.2 | Inoculation and symptom monitoring

In both ambient and saturation light gas exchange experiments, wheat spikes were inoculated with two contrasting strains in terms of

aggressiveness (MDC_Fg1 and MDC_FgU1; in decreasing order of aggressiveness; Fabre, Bormann, et al., 2019) or with water as control (Figure 1A). Fungal inoculations were performed in both experiments at mid-anthesis, with spore suspension obtained as previously described in Rocher et al. (2022). Spores were deposited with 10 μL of a spore solution at a concentration of 10^5 spores/mL in the floral cavity of all the spikelets of one spike. For the control samples, water was inoculated using the same procedure. For each experiment, a complete factorial design was produced with six biological replicates for each of the three treatment modalities, representing a total of 18 plants per experiment. Symptoms were scored using the 5-level rating scale given to each inoculated spikelet and described in Fabre, Vignassa, et al. (2019). The symptoms produced by MDC_Fg1 and MDC_FgU1 on the cultivar ‘Recital’ were assessed at 24, 48 and 72 hours post inoculation (hpi) in all biological replicates of each experiment.

2.1.3 | Gas exchange measurements

For both ambient and saturation light experiments, the measurements were performed on the same spikes of the same plants for each treatment. Pre-inoculation measurements were performed one day before mid-anthesis and then monitored at 24, 48 and 72 hpi to cover the FHB pre-symptomatic phase (Figure 1A). For both experiments and at each time point, measurements were performed during the day and night periods. Daytime measurements were performed 6 h after lamps were turned on in the growth chamber, while night-time measurements were realized 3 h after the lamps were switched off to assess the respiration level of the spikes.

Gas exchanges were measured using a portable gas-exchange system (Figure 1B-(3)) (LI-6400XT; LI-COR) associated with a light chamber specifically designed for spikes and three-dimensional organs (Figure 1B-(2)) (Fortineau & Bancal, 2018). In both light experiments, the reference CO_2 was set at 400 ppm and the flow at $600 \mu\text{mol s}^{-1}$. For the ambient light experiment, block temperatures were set at 21 and 17°C during the day and the night periods, respectively. For the saturation light experiment, block temperatures were set at 17°C for both day and night periods. For each spike, after a stabilization period of 200 s between the chamber closure and the first measurement, a series of seven measures every 10 s was performed. After the seventh measure, a match of the reference and sample infrared gas analyzers (IRGAs) was performed and subsequently used to correct any mismatch between the sample and reference cell when receiving the same air CO_2 . Spike's temperature was monitored throughout the measurements using a thermocouple inserted in the center of the spike between a spikelet and the rachis. Spike's temperature values are provided in the supplementary file 1. Ambient CO_2 concentration was measured every 5 s throughout the gas exchange measures using a $\text{CO}_2/\text{H}_2\text{O}$ gas analyzer (LI-840, LI-COR) and was used to take into account the variations of CO_2 concentration in the growth chamber along experiments (Supplementary file 1). To compute gas exchange values per unit area of each spike, experimented wheat

spikes were scanned, and their projected surface area was estimated using ImageJ software v.1.53e (Schneider et al., 2012).

2.1.4 | Statistical analyses of symptoms and gas exchange variables

All statistical analyses were conducted on R v4.1.1 (R Core Team, 2021). For all ecophysiological variables, the mean of the measurement series (seven successive measures) was used. All, except the absolute gross CO₂ assimilation rate (Pgross) at 72 hpi, were normalized according to the pre-inoculation point (X0). The LI6400 software uses numerous equations that directly provide results of physiological interest and are commonly calculated using many implicit equations. Our experiments are based on a customized chamber (Fortineau & Bancal, 2018), and these equations have been adapted following LICOR's indications. All adaptations and the gas exchange variables used in this study were computed according to the formulas detailed in the supplementary method. All data obtained during the experiments, including the normalized respiration rate (R/R0), normalized net CO₂ assimilation rate (Pnet/Pnet0), normalized gross CO₂ assimilation rate (Pgross/Pgross0), normalized total conductance to CO₂ (gtc/gtc0) and normalized intercellular CO₂ concentration (Ci/Ci0) are given in the supplementary file 1. A two-way repeated measures ANOVAs, with the kinetic factor nested within the biological replicate, were computed using the `anova_test` function of the `rstatix` package (Kassambara, 2022) to identify significant changes in all gas exchange variables as for the symptom scores. Pairwise comparisons were then performed using pairwise t-tests with the `pairwise-t-test` function of the `rstatix` package (Kassambara, 2022). Corrections for multiple testing were applied for all variables, except Pgross/Pgross0, using the Bonferroni adjustment method. The intensity of the Pnet/Pnet0 and Pgross/Pgross0 delta between 48 and 72 hpi was compared for MDC_Fg1 and MDC_FgU1 using pairwise t-tests with the `pairwise-t-test` function of the `rstatix` package (Kassambara, 2022). Light intensity and treatment effects were analyzed on the absolute Pgross at 72 hpi using a two-way ANOVA with the `anova_test` function of the `rstatix` package (Kassambara, 2022). Pairwise comparisons were performed using pairwise t-tests with the `pairwise-t-test` function of the `rstatix` package, and *p*-values were corrected for multiple testing using the Bonferroni adjustment method (Kassambara, 2022).

2.2 | Gene expression analysis

Gene expression data used in this study were retrieved from a previous RNAseq study (Rocher et al., 2024) available at NCBI under the accession PRJEB59062. The experiment was carried out with the wheat cultivar 'Recital' and three *F. graminearum* strains of contrasting aggressiveness MDC_Fg1, MDC_Fg13 and MDC_FgU1; in decreasing order of aggressiveness (Fabre, Bormann, et al., 2019). The samples were collected at 48, 72 and 96 hpi. Each treatment × time point condition was repeated four times (except for MDC_Fg13 × 72

hpi condition with three replicates). Plants were grown using the same procedure as described for the ecophysiological experiments. For each biological replicate, spore inoculation was performed on the six central spikelets of three synchronous flowering spikes (totalling 18 spikelets). For the mock samples, water was inoculated using the same procedure. Only inoculated spikelets were sampled for sequencing. The bioinformatics pipeline to obtain gene expression data is thoroughly detailed in Rocher et al. (2024). The filtered raw counts are provided (Supplementary File 2 - Table S2A).

2.2.1 | Retrieval of genes encoding functions involved in respiration, photosynthesis or stomatal movement

KEGG Orthology (KO) (Kanehisa & Goto, 2000) annotation of the High (HC) and Low Confidence (LC) of *Triticum aestivum* proteomes v1.1 (https://urgi.versailles.inra.fr/download/iwgsc/IWGSC_RefSeq_Annotations/v1.1/), was performed using GhostKOALA software with the “genus_prokaryotes + family_eukaryotes option” (Kanehisa et al., 2016). GhostKOALA results were then trimmed to keep only genes with an annotation generated from the plant kingdom. Respiration and Photosynthesis-associated KO lists were generated from the KEGG Modules part of the KEGG BRTE database (Kanehisa et al., 2006; https://www.genome.jp/kegg-bin/show_brite?ko00002.keg) to retrieve the corresponding genes. For stomatal movement-associated gene, Gene Ontology (GO) terms of the *Triticum aestivum* v1.1 genome were retrieved from ensembl (https://plants.ensembl.org/Triticum_aestivum/Info/Index) using the BiomaRt R interface (Durinck et al., 2009). GO terms were then used to build a wheat annotation orgdb R package using the `makeOrgPackage` function of the AnnotationForge R package (Carlson & Pagès, 2022). Following GO terms were used to retrieve wheat genes associated with stomatal movement: GO:1902456, GO:0090333. Gene functions were then retrieved from the UniProtKB database (Boutet et al., 2007). The wheat genes database established for this study is provided in Supplementary File 2 - Table S2B.

2.2.2 | Statistical analyses

Differential Expression analyses were conducted using the `DiffAnalysis_EdgeR` function of the DicoExpress script-based tool (Lambert et al., 2020), based on the EdgeR package (Robinson et al., 2010) and generating all the contrasts automatically for complex experimental designs. Only genes that were differentially expressed (DE) in response to the three strains in comparison to the control and predicted to be involved in respiration, photosynthesis, or stomatal movement were used in this study. Prior to expression pattern characterization, the raw count values were normalized using the regularized logarithm transformation (rlog) implemented in the DESeq2 package (Love et al., 2014). Then, a z-score transformation was applied to the normalized count values, and gene expression patterns were

described using heat maps using the Pheatmap package (Kolde, 2019). The genes and samples were clustered using the ward.D2 agglomeration method was applied to the Euclidean distance matrices (Murtagh & Legendre, 2014). In order to highlight the robustness and repetitiveness of our RNA-seq data, the DEGs identified in this study were compared to the results of another RNA-seq data set obtained in the same growth chamber and using the same wheat genotype, 'Recital', that was infected by the strain MDC_Fg1, strain also used in this study. All the details concerning this RNA-seq data-set are described under the name HostV in our previously published paper Rocher et al. (2024). Only DEGs from Recital infected by MDC_Fg1 in comparison to the control condition were considered. The consistency was checked by comparing gene log2FC in both RNA-seq experiments.

3 | RESULTS

3.1 | *In situ* impacts of FHB on ecophysiological parameters of photosynthesis and respiration

Consequences of *F. graminearum* development in the spike's physiological functioning were assessed using two *F. graminearum* strains of contrasting aggressiveness, MDC_Fg1 (the most aggressive strain) and MDC_FgU1 (the less aggressive one), as previously reported in Fabre, Bormann et al. 2019. In our study, the symptom survey confirmed this previous work with clear differences as early as 48 hpi between MDC_Fg1 and MDC_FgU1 (Figure 2). While a significant increase was observed in the induced symptoms for both strains

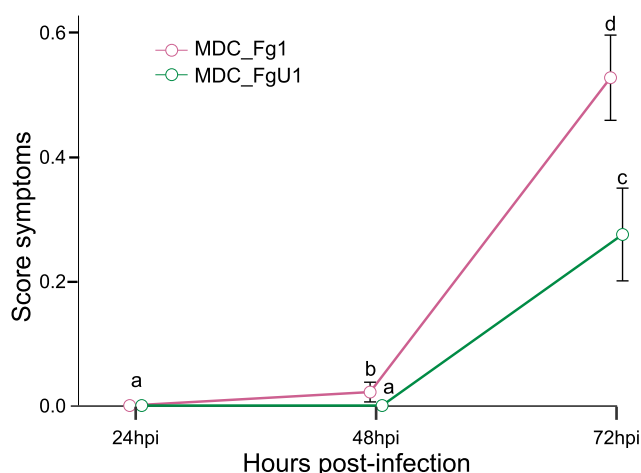


FIGURE 2 Symptom development induced by the two *F. graminearum* strains of contrasting aggressiveness. Line plots represent the score symptoms observed at 24, 48 and 72 hpi for MDC_Fg1 (pink) and MDC_Fg13 (green). The score symptoms measured during both gas exchange experiments were used (12 replicates). Error bars represent the 95% confidence intervals. Significance threshold: p-value<0.05.

between 48 and 72 hpi, MDC_Fg1 induced symptoms earlier and with more intensity than MDC_FgU1, with an average score symptom at 72 hpi that was twice as severe with MDC_Fg1 compared to MDC_FgU1.

3.1.1 | FHB induced a strong increase in the spike's respiration rate

In response to MDC_Fg1 and MDC_FgU1 infection, a significant increase in the normalized respiration rate (R/R_0) was monitored at the whole spike level along with the infection progress for both ambient and saturation light experiments (Figure 3A and Supplementary File 3 - Table S3-1). In both experiments, R/R_0 hardly varied in the control plants. A slight increase of the R/R_0 was detected between 24 and 72 hpi only in the ambient light experiment (Supplementary File 3 - Table S3-1). The inoculation of MDC_Fg1 and MDC_FgU1 induced a significantly higher R/R_0 in the infected spikes than in the control ones at 48 hpi and 72 hpi, in both experiments (Figure 3A). Significant strain-dependent responses were also detected in the ambient experiment, where MDC_Fg1 induced a higher R/R_0 than MDC_FgU1 at both 48 hpi and 72 hpi.

3.1.2 | FHB resulted in a decrease in the spike's CO_2 assimilation rate

Control samples did not display any significant changes in the normalized net CO_2 assimilation rate (P_n/P_{n0}) in both experiments, while the inoculation of MDC_Fg1 and MDC_FgU1 induced a significant drop of the P_n/P_{n0} between 48 and 72 hpi, regardless of the light intensity (Supplementary File 3 - Table S3-2). No significant differences were observed between conditions at both 24 and 48 hpi, but both strains induced a significantly lower P_n/P_{n0} than control plants at 72 hpi in both light experiments (Figure 3B). No significant strain-dependent changes were detected between MDC_Fg1- and MDC_FgU1-inoculated spikes. Similar trends were observed in the normalized gross CO_2 assimilation rate (P_{gross}/P_{gross0}), with no clear strain-dependent trends (Figure 3C). A significant drop of P_{gross}/P_{gross0} was observed between 48 and 72 hpi for both strains, while it remained stable in the control spikes (Supplementary File 3 - Table S3-3). The t-test comparison of the 72–48 hpi delta between P_{net}/P_{net0} and P_{gross}/P_{gross0} showed that the drop was significantly higher for P_n/P_{n0} regardless of the inoculated strain. While infection with MDC_Fg1 induced a significantly higher P_{gross}/P_{gross0} in spike than the infection with MDC_FgU1 at 24 hpi in the ambient light experiment only, no differences of P_{gross}/P_{gross0} were detected between the three conditions at 48 hpi in both experiments. At 72 hpi, the MDC_Fg1-inoculated spikes displayed a significantly lower P_{gross}/P_{gross0} than the control spikes in both experiments, while the response to MDC_FgU1 was significantly different to the controls in the

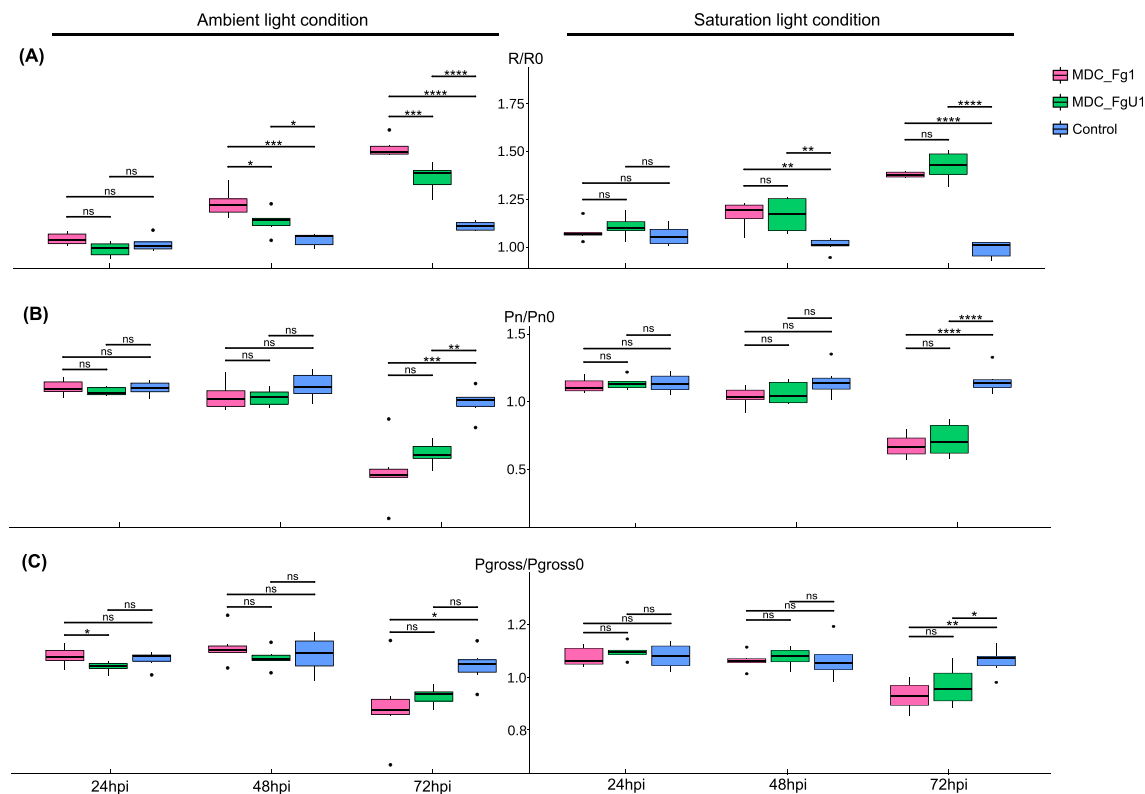


FIGURE 3 Normalized respiration rate (R/R0) (A), normalized net CO₂ assimilation rate (Pn/Pn0) (B) and normalized gross CO₂ assimilation rate (Pgross/Pgross0) (C) of 'Recital' spikes measured in response to treatment along the infection progress in both ambient light and saturation light conditions. Boxplots are shown at 24, 48 and 72 hpi after the inoculation of MDC_Fg1 (pink), MDC_FgU1 (green) and for controls (blue) relatively to the pre-inoculation point. Asterisks indicate a significant difference between two treatment modalities at one given time point while ns indicate a non-significant difference. Significance threshold: Bonferroni adjusted p -value < 0.05.

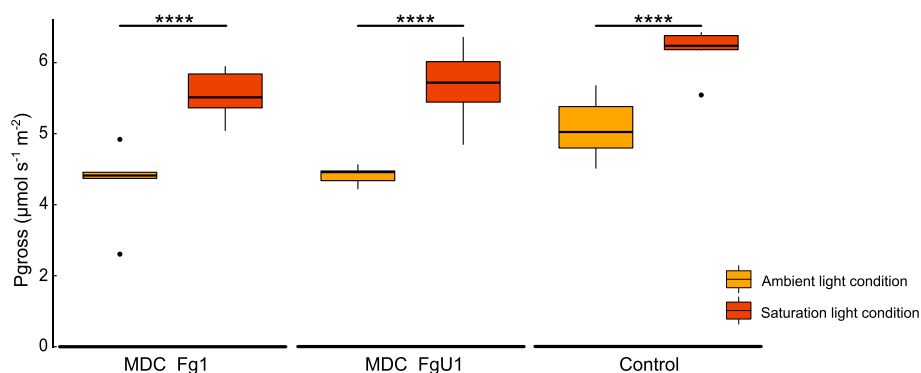


FIGURE 4 Absolute gross CO₂ assimilation rate (Pgross) of 'Recital' spikes measured at 72 hpi in response to treatment and light conditions. Boxplots represent the gross CO₂ assimilation rate of the spikes (Pgross) measured at 72 hpi after the inoculation of MDC_Fg1 (upper left panel), MDC_FgU1 (upper right panel) and water (bottom panel) for controls in ambient light (orange) and saturation light (reddish orange) conditions. Asterisks indicate a significant difference between the two light modalities. Significance threshold: Bonferroni adjusted p -value < 0.05.

saturation light experiment only (Figure 3C). Finally, the absolute level of Pgross, was significantly higher (+1.2 μmol s⁻¹ m⁻²) in the saturation light condition than in the ambient light (Figure 4). No interaction effect was detected between the light intensity and the treatment factors, indicating a generic response to light intensity independent of treatments.

3.1.3 | FHB infection did not change the conductance to CO₂

The effects of FHB on the stomatal aperture were investigated using the normalized total conductance to CO₂ (g_{tc}/g_{tc0}). The only significant change observed was a significant reduction between 48 and

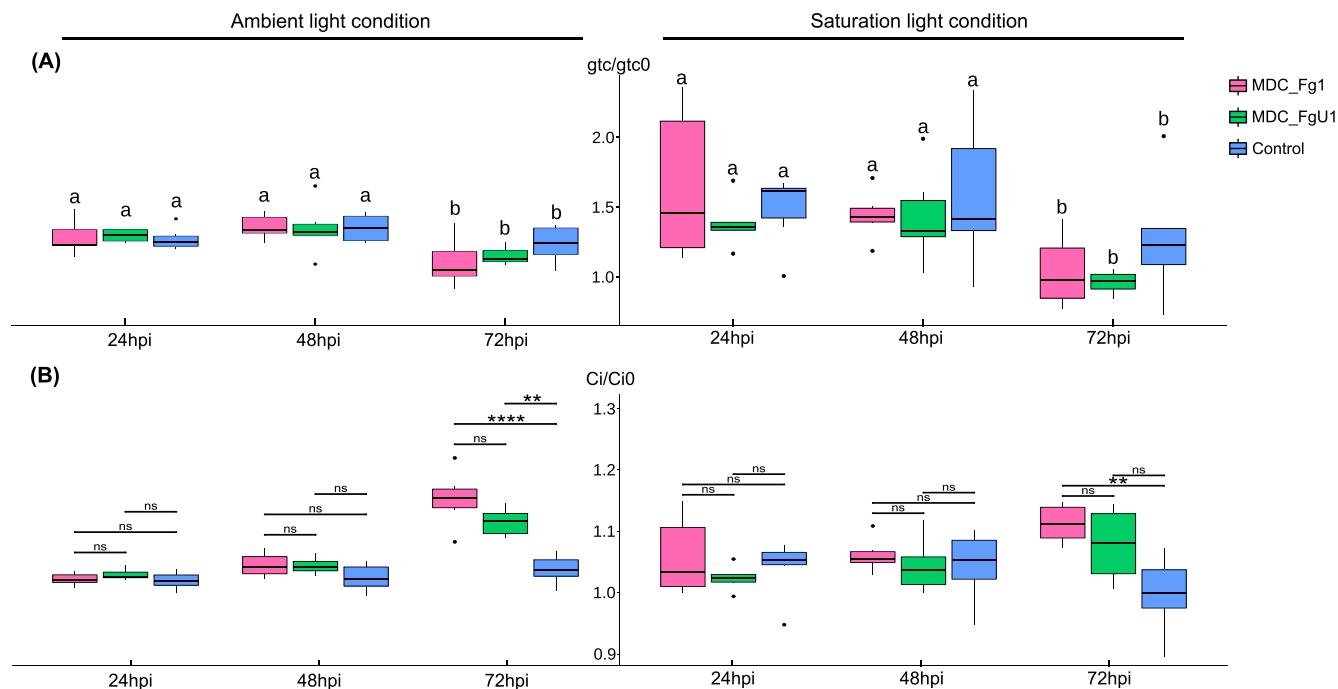


FIGURE 5 Normalized total conductance to CO₂ (gtc/gtc0) (A) and normalized inter-cellular CO₂ concentration (Ci/Ci0) (B) of ‘Recital’ spikes measured in response to treatment along the infection progress in both ambient light and saturation light conditions. Boxplots are shown at 24 hpi, 48 hpi and 72 hpi after the inoculation of MDC_Fg1 (pink), MDC_FgU1 (green) and for controls (blue) relatively to the pre-inoculation point. Letters indicate a significant difference between time points. Asterisks indicate a significant difference between two treatment modalities at one given time point while ns indicate a non-significant difference. Significance threshold: Bonferroni adjusted p-value < 0.05.

72 hpi in both experiments under all conditions, including control, but without any effect of the treatments (Figure 5A). The variations of the normalized CO₂ concentration in the sub-stomatal internal cavities (Ci/Ci0) were sharper in the ambient light experiment than in the saturation light experiment (Supplementary File 3 - Table S3-4). In the ambient light experiment, the inoculation of MDC_Fg1 and MDC_FgU1 induced a significant increase of the Ci/Ci0 in spikes along with the infection duration while it remained stable in the controls (Supplementary File 3 - Table S3-4A). In the saturation light experiment, only MDC_Fg1-inoculated spikes displayed a significant increase of the Ci/Ci0 between 48 and 72 hpi, while a significant decrease was observed in the control spikes (Supplementary File 3 - Table S3-4B). In both experiments, no differences of Ci/Ci0 were detected between conditions at 24 and 48 hpi (Figure 5B). At 72 hpi, the Ci/Ci0 was significantly higher in response to MDC_Fg1 and MDC_FgU1 than in the control spikes in the ambient light condition, while only MDC_Fg1 inoculation induced a higher Ci/Ci0 than the control spikes in the saturation light experiment (Figure 5B).

3.2 | FHB impacts on the expression of photosynthesis- and respiration-related genes

The consequences of *F. graminearum* inoculation on the wheat genes involved in photosynthesis- and respiration-associated processes were studied by retrieving all the FHB-responsive genes that were systematically regulated in the ‘Recital’ cultivar when facing

independently three *F. graminearum* strains of contrasting aggressiveness (Rocher et al., 2024). This experiment included the two strains used in the ecophysiological experiments, MDC_Fg1 and MDC_FgU1, and was completed by a third, MDC_Fg13, displaying intermediate aggressiveness (Fabre, Bormann, et al., 2019; Rocher et al., 2024).

A total of 445 unique genes involved in photosynthesis, respiration and stomatal functioning were found differentially expressed in response to the three *F. graminearum* strains. Among them, 62 genes were annotated in both photosynthesis and respiration processes. To highlight the consistency and reproducibility of our DE results, we compared the responsive patterns of this DEG list with results from another independent RNA-seq study performed in the same growth chamber with the same wheat genotype and the strain MDC_Fg1 study (Rocher et al., 2024). Among the 445 DEGs, 383 (86%) were found differentially expressed in both RNA-seq experiments, among which 87, 100 and 100% displayed the same responsive pattern at 48, 72 and 96 hpi, respectively. This high degree of reproducibility between two independent RNA-seq experiments clearly emphasizes the tremendous robustness of the identified gene regulations (Supplementary Table S2C).

3.2.1 | The expression of the photosynthesis-associated genes was widely decreased in response to FHB

A total of 256 genes involved in photosynthesis-associated processes were found to be significantly impacted by each of the fungal strains

(Supplementary file 4 - Table S4A, “FHB responsive photosynthesis-genes”, FHB-Photo-genes). The Hierarchical Ascendant Clustering (HAC) clearly discriminated the infected modalities from the control as well as the infection stages for the infected modalities rather than

distinguishing the fungal strains (Figure 6A). Around 81% (207 genes) of this gene set displayed higher expression in the control modality than in the infected ones regardless of the inoculated strain (Cluster C1, Table 1A), with a strong expression drop between 48 and 72 hpi

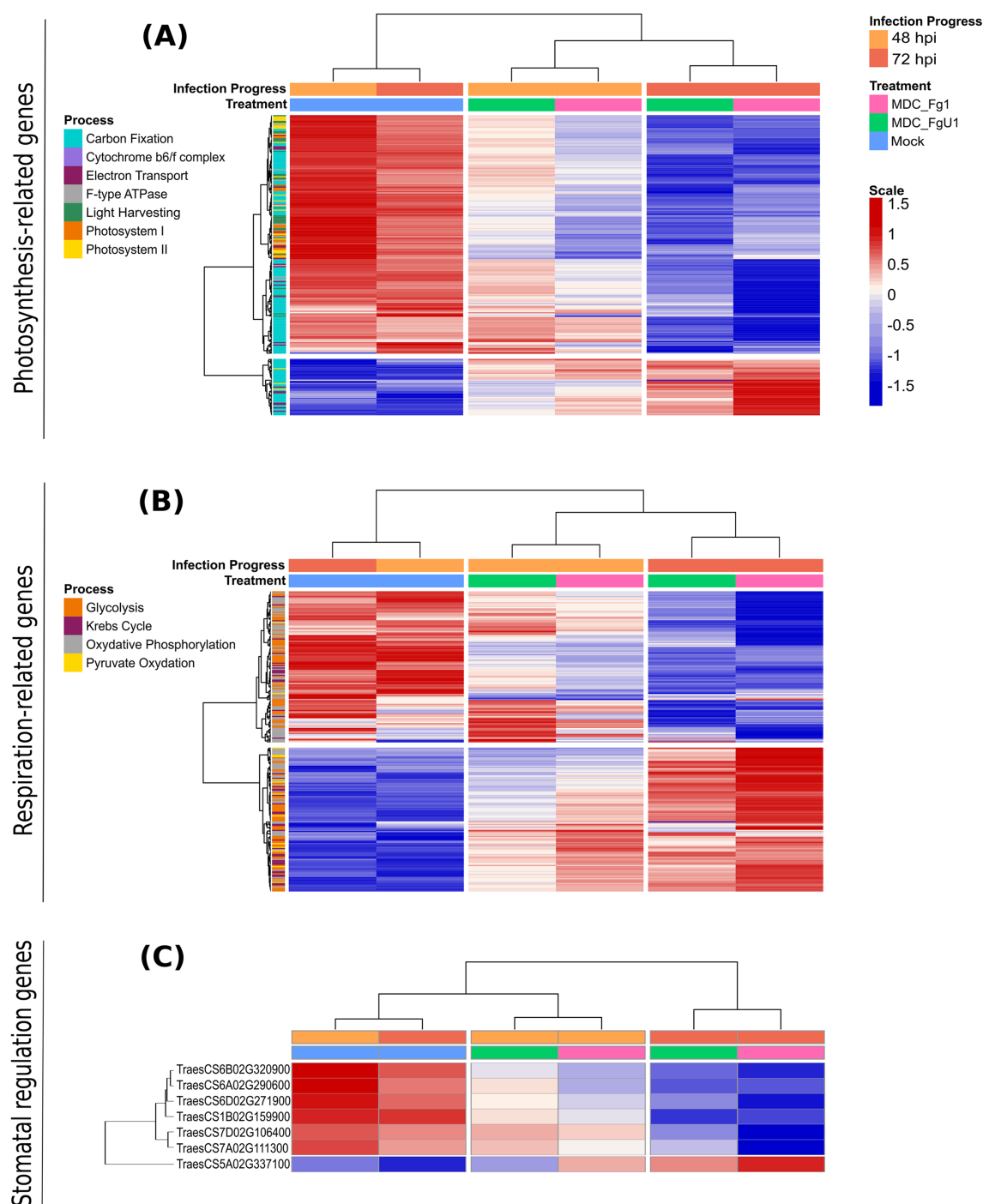


FIGURE 6 Expression patterns of the FHB-responsive genes involved (A) in the photosynthesis-related processes, (B) in the respiration-related processes and (C) in stomatal regulation. Expression profiles are given for the wheat cultivar ‘Recital’ facing the two strains of contrasting aggressiveness, MDC_Fg1 and MDC_FgU1. Genes and sample data sets were grouped using a Hierarchical Ascendant Clustering based on Ward’s minimum variance method and using the z-score transformed gene expression values. Heatmap color scales represent the z-score values of the genes. The clustering on top of the heatmaps represents the experimental conditions, labeled according to the both the treatment (Mock, MDC_Fg1 and MDC_FgU1) and the infection delay (48 hpi and 72 hpi). On the left side of the heatmaps, the genes were colored according to the process in which they are involved or labeled with their accession number.

in the infected spikes (Figure 6A). All the genes involved in the “Light harvesting” (30 genes), “Photosystem I” (19 genes), “F-type ATPase” (9 genes) and “Cytochrome b6/f complex” (1 gene) processes displayed less expressed transcripts in response to FHB (Table 1A). Likewise, about 90% (22 genes), 75% (110 genes) and 70% (16 genes) of the genes involved in “Photosystem II”, “Carbon Fixation” and “Electron Transport” proved also to be less expressed in response to FHB. On the opposite, only 49 genes displayed lower expression levels in the control modality than in the infected ones (Cluster C2, Table 1A), with a strong increase of their expression between 48 hpi and 72 hpi in the infected spikes, whatever the fungal strain. Only one gene, TraesCS5B02G516600, involved in the “Photosystem II” process and belonging to the first clustering group, was differentially expressed between MDC_Fg1- and MDC_FgU1-infected spikes.

TABLE 1 Resume of the photosynthesis- (A) and respiration-associated (B) processes affected by FHB at the molecular level. Concerning the photosynthesis-associated processes (A), the cluster C1 represents the genes repressed in response to FHB compared to control plants and the cluster C2 represents the genes induced in response to FHB compared to control plants. Concerning the respiration-associated processes (B), the cluster C1 represents the genes repressed in response to FHB compared to control plants and the cluster C2 represents the genes induced in response to FHB compared to control plants.

A. Biological process	Cluster	Gene number
Carbon fixation	C1	110
	C2	39
Cytochrome b6/f complex	C1	1
	C2	0
Electron transport	C1	16
	C2	7
F-type ATPase	C1	9
	C2	0
Light harvesting, Chlorophyll protein	C1	30
	C2	0
Photosystem I	C1	19
	C2	0
Photosystem II	C1	22
	C2	3
B. Biological process	Cluster	Gene number
Glycolysis	C1	50
	C2	48
Krebs cycle	C1	17
	C2	26
Pyruvate oxidation	C1	56
	C2	33
Oxidative phosphorylation	C1	2
	C2	12

3.2.2 | FHB-induced regulations in respiration-related genes showed a multifaceted response

A total of 244 genes involved in the respiration-associated processes were found to be regulated upon FHB development (Supplementary file 4 - Table S4B, “FHB responsive respiration-genes”, FHB-Resp-genes). As shown for photosynthesis-related genes, the HAC of the mRNA accumulation of the FHB-Resp-genes clearly discriminated the control plants from the infected ones as well as the infection stage for the infected modalities, while the strain aggressiveness displayed only minor effects on the variances (Figure 6B). FHB impacts on this gene set evidenced two balanced groups. The first group, gathering 125 genes, displayed FHB-Resp-genes with decreasing mRNA expression in the infected plants (Cluster C1, Table 1B), depicting a strong expression drop between 48 and 72 hpi (Figure 6B). This group included most of the genes involved in the “Oxidative Phosphorylation” process (~65% of the set) (Table 1B). On the opposite, the second group, gathering 119 genes, displayed FHB-Resp-genes with increasing mRNA expression in the infected plants (Cluster C2, Table 1B), depicting a strong expression burst between 48 and 72 hpi. This group included most of the genes involved in the “Krebs cycle” and “Pyruvate oxidation” processes (~70 and ~85% of the gene set, respectively) (Table 1B). Regarding the genes involved in the “Glycolysis” process, they were equally distributed in the two groups, with 50 and 48 genes displaying, respectively, lower and higher expression levels in the infected plants as compared to the control ones (Table 1B). Only two genes (TraesCS1D02G215900 and TraesCS3B02G199500) belonging to the second group and involved in the “Glycolysis” and the “Krebs cycle” processes, respectively, were differentially expressed between MDC_Fg1- and MDC_FgU1-infected spikes.

3.2.3 | The expression of genes involved in stomatal movement was mainly repressed in response to FHB

A total of 7 genes involved in stomatal movement-associated processes were found to be significantly impacted by each of the fungal strains (“FHB responsive stomatal genes”, FHB-Sto genes). The HAC of the mRNA accumulation of these genes clearly discriminated the infected conditions from the controls as well as the infection stages for the infected modalities rather than the fungal strains (Figure 6C). Except for one, all the FHB-Sto-genes displayed a higher expression in the control spikes than in the infected ones, with a strong expression drop between 48 and 72 hpi in the infected conditions (Figure 6C). Among the down-regulated functions in response to FHB, 3 homeologs coding for “chloroplast calcium-sensing receptors”, 2 homeologs coding for “mitogen-activated protein kinases” and 1 gene coding for a “key zinc finger transcription factor gene” were found (Supplementary File 4 - Table S4C). The only up-regulated gene in response to FHB coded for a “phospholipase D” (Supplementary File 4 - Table S4C).

4 | DISCUSSION

Taking advantage of two *F. graminearum* strains of contrasting aggressiveness, the impacts of FHB on the spike's basal functioning were assessed using complementary approaches at the ecophysiological and molecular levels. This included the characterization of the gas exchanges of wheat spikes during the infection progress using a specific device for three-dimensional organs, along with the profiling of the expression changes of photosynthesis- and respiration-associated genes.

4.1 | Impairments of photosynthetic parameters during FHB are mediated by a specific remodelling of gene expression and are independent of symptomatic tissue damages

Measurements of the CO₂ assimilation rate, especially upon the saturation light intensity, clearly revealed an impairment of photosynthesis at both net and gross levels. Changes were especially sharp between 48 and 72 hpi and occurred independently of strain aggressiveness. The intense drop of the net CO₂ assimilation rate at 72 hpi was primarily linked to the strong increase in the respiration rate observed between 48 and 72 hpi. However, the gross assimilation rate also decreased, albeit to a smaller extent, which suggests that FHB impact on the net photosynthesis rate can be a combination of a decrease in the gross photosynthesis rate and an increase in the respiration rate. The total conductance to CO₂ largely increased from 0 to 24 hpi in both control and inoculated spikes. This ontogenic change could be attributed to the glume aperture that occurs at anthesis. Furthermore, FHB did not affect the total conductance to CO₂, suggesting that neither the stomatal CO₂ diffusion nor the cuticular permeability to CO₂ were altered along the infection progress. Consequently, the drop in the photosynthesis during FHB could not be related to a reduced CO₂ influx in the tissues; thereby, the increased Ci within the spike could be a direct consequence of the drop in the net CO₂ assimilation rate, assuming a stable mesophyll conductance. At the transcriptional level, FHB infection demonstrated both down- and up-regulations in gene expression, suggesting that spike functioning is still adjusting upon the time course of infection. However, FHB impact is especially characterized by a sharp down-regulation of the genes associated with the photochemical and biochemical phases of photosynthesis, which has been observed independently of the strain's aggressiveness. Such regulation in photosynthesis-associated processes corroborates previous FHB experiments that demonstrated (i) a strong abundance decrease of the proteins involved in light harvesting, photosystems and electron transport chain between 48 hpi and 72 hpi (Fabre, Vignassa, et al., 2019) and (ii) similar responses when the wheat cultivar is facing the same two *F. graminearum* strains we inoculated (Fabre, Bormann, et al., 2019). In our study, stomatal closure regulation appeared also concurrently altered in response to FHB, suggesting that stomatal closure was partly impaired upon infection. For instance, the three genes encoding chloroplast calcium-sensing receptors (CAS) were sharply

down-regulated upon FHB, while they are known to induce stomatal closure in response to extracellular calcium stimuli (Li et al., 2022). Besides their well characterized role in drought stress tolerance, CAS are also key components of the PAMP-triggered immunity, the salicylic acid synthesis, involved in immunity against biotrophic pathogens, but also in chloroplast-nucleus communication under biotic stress (Medina-Puche et al., 2020).

Taken together, our results suggest that the observed decrease in photosynthesis was neither a consequence of the symptom development nor an alteration of the stomatal regulation but the result of a direct or indirect alteration of the photochemical and biochemical processes. In line with our conclusions, a previous study demonstrated that the genes involved in stomatal closure were not induced in response to FHB in the susceptible cultivar 'Rebelde' and that the photosynthetic efficiency was altered at 72 hpi (Francesconi & Balestra, 2020). Similar results were also obtained in other wheat pathosystems, such as in *Septoria tritici* blotch (Robert et al., 2006), in leaf rust (Carretero et al., 2011) or in wheat blast (Debona et al., 2014). Another example in rice leaves has shown that infection with *Monographella albescens* resulted in a significant photosynthesis decrease in asymptomatic tissue or prior symptom development, which was mainly associated with a decrease in light capture (Tatagiba et al., 2015). Finally, despite the measurable impairment of the photosynthesis processes during FHB, wheat spike's tissues still responded to variations of light intensity, suggesting that chloroplasts remained partly functional even upon symptom appearance.

4.2 | Increase in respiration rate upon FHB is not only explained by the regulation of plant gene expression

FHB infection clearly induced a strong increase in the respiration rate in 'Recital' spikes that could be associated with a strong energy demand due to an accelerated metabolic activity or to the setup of plant defences (Major et al., 2010; Debona et al., 2014; Gramig & Harris, 2015). However, contrary to the photosynthetic processes, no clear links have been observed between the expression of the genes involved in the respiration pathways and the measured respiration rate. This may be the direct consequence of the highly flexible nature of plant respiration that can employ alternative pathways that bypass the conventional ones (Plaxton & Podestá, 2006; van Dongen et al., 2011). For instance, plants are able to use substrates other than pyruvate, such as malate and formate but also amino and fatty acids (Plaxton & Podestá, 2006). One limitation of this study is that FHB effects on the photorespiration processes were not assessed, while it is known to be involved in plant defences against pathogens through H₂O₂ accumulation (Sørhagen et al., 2013).

To conclude, combining the molecular characterization of a pathosystem with ecophysiological methods allowed us to refine our understanding of how the host's processes impacted along with the infection progress. Gas exchange measurements have proven to be a powerful tool to finely phenotype complex traits, such as

susceptibility to plant pathogens, by going beyond the use of traditional variables such as score symptom monitoring. The physiological results obtained in this study corroborated the genericity of wheat's responses to FHB early stages that were previously revealed at the transcriptome level by the conservation of effectors between different strains (Rocher et al., 2022) and the conservation of the wheat cultivar 'Recital' responses to those same strains (Rocher et al., 2024). The CO₂ assimilation and diffusion responses to FHB were consistent with the transcriptomic responses observed for photosynthesis-related genes, both methods indicating an alteration of the photo- and biochemical processes of the photosynthetic apparatus, which do not appear to be directly associated with symptom development. Finally, the ecophysiological approach has proven to be particularly effective in determining the impact of *F. graminearum* on respiration, a process for which the characterization at the transcriptome scale was not sufficient and difficult due to the complexity of the network of actors involved.

AUTHOR CONTRIBUTIONS

LB and FR designed the experiments. FR, GP and AF performed the experiments. FR, PB and LB analyzed the data. LB and FR wrote the first manuscript version. PB, AF, PL and TL reviewed the manuscript, and all authors accepted the final version of the manuscript.

ACKNOWLEDGEMENTS

The authors thank Richard Blanc for its valuable help during experiments as well as Florence Cambon and Olivier Soudière for their assistance in RNA extraction and *Fusarium graminearum* spore production. This research and PhD grant (FR) were funded by the Region Auvergne-Rhône-Alpes and the FEDER supports. Transcriptomics was supported by the Agence Nationale de la Recherche of the French government (NewMyco project, ANR-15-CE21-0010). The authors also acknowledge the support received from the Agence Nationale de la Recherche of the French government through the program "Investissements d'Avenir" (16-IDEX-0001 CAP 20-25; International Research Center on Sustainable AgroEcosystems and CAP2025 Academy).

DATA AVAILABILITY STATEMENT

The data and the analyses that supports the findings of this study are available in the supplementary material of this article.

ORCID

Ludovic Bonhomme  <https://orcid.org/0000-0001-9410-0827>

REFERENCES

- Argyris, J., van Sanford, D., & TeKrony, D. (2003). *Fusarium graminearum* Infection during Wheat Seed Development and Its Effect on Seed Quality. *Crop Science*, 43(5), 1782–1788. <https://doi.org/10.2135/cropsci2003.1782>
- Bai, G., Su, Z., & Cai, J. (2018). Wheat resistance to *Fusarium* head blight. *Canadian Journal of Plant Pathology*, 40(3), 336–346. <https://doi.org/10.1080/07060661.2018.1476411>
- Boutet, E., Lieberherr, D., Tognolli, M., Schneider, M., & Bairoch, A. (2007). UniProtKB/Swiss-Prot. In D. Edwards (Ed.), *Plant Bioinformatics: Methods and Protocols* (pp. 89–112). Humana Press. https://doi.org/10.1007/978-1-59745-535-0_4
- Boyacioglu, D., & Hettiarachchy, N. S. (1995). Changes in some biochemical components of wheat grain that was infected with *Fusarium graminearum*. *Journal of Cereal Science*, 21(1), 57–62. [https://doi.org/10.1016/S0733-5210\(95\)80008-5](https://doi.org/10.1016/S0733-5210(95)80008-5)
- Brauer, E. K., Balcerzak, M., Rocheleau, H., Leung, W., Scherthaner, J., Subramaniam, R., & Ouellet, T. (2020). Genome Editing of a Deoxynivalenol-Induced Transcription Factor Confers Resistance to *Fusarium graminearum* in Wheat. *Molecular Plant-Microbe Interactions*, 33(3), 553–560. <https://doi.org/10.1094/MPMI-11-19-0332-R>
- Caplan, J. L., Kumar, A. S., Park, E., Padmanabhan, M. S., Hoban, K., Modla, S., Czymmek, K., & Dinesh-Kumar, S. P. (2015). Chloroplast Stromules Function during Innate Immunity. *Developmental Cell*, 34(1), 45–57. <https://doi.org/10.1016/j.devcel.2015.05.011>
- Carlson, M., & Pagès, H. (2022). AnnotationForge: Tools for building SQLite-based annotation data packages. (Version Bioconductor version: Release (3.15)) [Computer software]. [10.18129/B9.bioc.AnnotationForge](https://doi.org/10.18129/B9.bioc.AnnotationForge)
- Carretero, R., Bancal, M. O., & Miralles, D. J. (2011). Effect of leaf rust (*Puccinia triticina*) on photosynthesis and related processes of leaves in wheat crops grown at two contrasting sites and with different nitrogen levels. *European Journal of Agronomy*, 35(4), 237–246. <https://doi.org/10.1016/j.eja.2011.06.007>
- Chen, Y., Kistler, H. C., & Ma, Z. (2019). *Fusarium graminearum* Trichothecene Mycotoxins: Biosynthesis, Regulation, and Management. *Annual Review of Phytopathology*, 57, 15–39. <https://doi.org/10.1146/annurev-phyto-082718-100318>
- Chhabra, B., Tiwari, V., Gill, B. S., Dong, Y., & Rawat, N. (2021). Discovery of a susceptibility factor for *Fusarium* head blight on chromosome 7A of wheat. *Theoretical and Applied Genetics*, 134(7), 2273–2289. <https://doi.org/10.1007/s00122-021-03825-y>
- Colombatti, F., Gonzalez, D. H., & Welchen, E. (2014). Plant mitochondria under pathogen attack: A sigh of relief or a last breath? *Mitochondrion*, 19, 238–244. <https://doi.org/10.1016/j.mito.2014.03.006>
- Dahl, B., & Wilson, W. W. (2018). Risk premiums due to *Fusarium* Head Blight (FHB) in wheat and barley. *Agricultural Systems*, 162, 145–153. <https://doi.org/10.1016/j.agry.2018.01.025>
- Darino, M., Jaiswal, N., Darna, R., Kroll, E., Urban, M., Xiang, Y., Srivastava, M., Kim, H.-S., Myers, A., Scofield, S. R., Innes, R. W., Hammond-Kosack, K. E., & Helm, M. (2024). The *Fusarium graminearum* effector protease FgTPP1 suppresses immune responses and facilitates *Fusarium* Head Blight Disease (p. 2024.08.30.610543). *bioRxiv*. <https://doi.org/10.1101/2024.08.30.610543>
- de Torres Zabala, M., Littlejohn, G., Jayaraman, S., Studholme, D., Bailey, T., Lawson, T., Tillich, M., Licht, D., Bölter, B., Delfino, L., Truman, W., Mansfield, J., Smirnov, N., & Grant, M. (2015). Chloroplasts play a central role in plant defence and are targeted by pathogen effectors. *Nature Plants*, 1(6), 1–10. <https://doi.org/10.1038/nplants.2015.74>
- Debona, D., Rodrigues, F. Á., Rios, J. A., Martins, S. C. V., Pereira, L. F., & DaMatta, F. M. (2014). Limitations to Photosynthesis in Leaves of Wheat Plants Infected by *Pyricularia oryzae*. *Phytopathology*, 104(1), 34–39. <https://doi.org/10.1094/PHYTO-01-13-0024-R>
- Durinck, S., Spellman, P. T., Birney, E., & Huber, W. (2009). Mapping identifiers for the integration of genomic datasets with the R/Bioconductor package biomaRt. *Nature Protocols*, 4(8), 1184–1191. <https://doi.org/10.1038/nprot.2009.97>
- Engelhardt, S., Stam, R., & Hückelhoven, R. (2018). Good Riddance? Breaking Disease Susceptibility in the Era of New Breeding Technologies. *Agronomy*, 8(7), Article 7. <https://doi.org/10.3390/agronomy8070114>
- Fabre, F., Bormann, J., Urbach, S., Roche, S., Langin, T., & Bonhomme, L. (2019). Unbalanced Roles of Fungal Aggressiveness and Host Cultivars

- in the Establishment of the Fusarium Head Blight in Bread Wheat. *Frontiers in Microbiology*, 10. <https://doi.org/10.3389/fmicb.2019.02857>
- Fabre, F., Rocher, F., Alouane, T., Langin, T., & Bonhomme, L. (2020). Searching for FHB Resistances in Bread Wheat: Susceptibility at the Crossroad. *Frontiers in Plant Science*, 11. <https://doi.org/10.3389/fpls.2020.00731>
- Fabre, F., Vignassa, M., Urbach, S., Langin, T., & Bonhomme, L. (2019). Time-resolved dissection of the molecular crosstalk driving Fusarium head blight in wheat provides new insights into host susceptibility determinism. *Plant, Cell & Environment*, 42(7), 2291–2308. <https://doi.org/10.1111/pce.13549>
- Figueroa, M., Ortiz, D., & Henningsen, E. C. (2021). Tactics of host manipulation by intracellular effectors from plant pathogenic fungi. *Current Opinion in Plant Biology*, 62, 102054. <https://doi.org/10.1016/j.pbi.2021.102054>
- Fortineau, A., & Bancal, P. (2018). An innovative light chamber for measuring photosynthesis by three-dimensional plant organs. *Plant Methods*, 14(1), 21. <https://doi.org/10.1186/s13007-018-0288-5>
- Francesconi, S., & Balestra, G. M. (2020). The modulation of stomatal conductance and photosynthetic parameters is involved in Fusarium head blight resistance in wheat. *PLOS ONE*, 15(6), e0235482. <https://doi.org/10.1371/journal.pone.0235482>
- Garcia-Ruiz, H., Szurek, B., & Van den Ackerveken, G. (2021). Stop helping pathogens: Engineering plant susceptibility genes for durable resistance. *Current Opinion in Biotechnology*, 70, 187–195. <https://doi.org/10.1016/j.copbio.2021.05.005>
- Garvin, D. F., Porter, H., Blankenheim, Z. J., Chao, S., & Dill-Macky, R. (2015). A spontaneous segmental deletion from chromosome arm 3DL enhances Fusarium head blight resistance in wheat. *Genome*, 58(11), 479–488. <https://doi.org/10.1139/gen-2015-0088>
- Gorash, A., Armoniené, R., & Kazan, K. (2021). Can effectomics and loss-of-susceptibility be exploited for improving Fusarium head blight resistance in wheat? *The Crop Journal*, 9(1), 1–16. <https://doi.org/10.1016/j.cj.2020.06.012>
- Gordon, C. S., Rajagopalan, N., Risseuw, E. P., Surpin, M., Ball, F. J., Barber, C. J., Buhrow, L. M., Clark, S. M., Page, J. E., Todd, C. D., Abrams, S. R., & Loewen, M. C. (2016). Characterization of Triticum aestivum Abscissic Acid Receptors and a Possible Role for These in Mediating Fusarium Head Blight Susceptibility in Wheat. *PLOS ONE*, 11(10), e0164996. <https://doi.org/10.1371/journal.pone.0164996>
- Gortari, F., Guimet, J. J., & Graciano, C. (2018). Plant-pathogen interactions: Leaf physiology alterations in poplars infected with rust (*Melampsora medusae*). *Tree Physiology*, 38(6), 925–935. <https://doi.org/10.1093/treephys/tpx174>
- Goswami, R. S., & Kistler, H. C. (2004). Heading for disaster: Fusarium graminearum on cereal crops. *Molecular Plant Pathology*, 5(6), 515–525. <https://doi.org/10.1111/j.1364-3703.2004.00252.x>
- Gramig, G. G., & Harris, M. O. (2015). Plant Photosynthetic Responses During Insect Effector-Triggered Plant Susceptibility and Immunity. *Environmental Entomology*, 44(3), 601–609. <https://doi.org/10.1093/ee/nvv028>
- Hales, B., Steed, A., Giovannelli, V., Burt, C., Lemmens, M., Molnár-Láng, M., & Nicholson, P. (2020). Type II Fusarium head blight susceptibility conferred by a region on wheat chromosome 4D. *Journal of Experimental Botany*, 71(16), 4703–4714. <https://doi.org/10.1093/jxb/eraa226>
- Horst, R. J., Doehlemann, G., Wahl, R., Hofmann, J., Schmiedl, A., Kahmann, R., Kasper, J., Sonnewald, U., & Voll, L. M. (2010). Ustilago maydis Infection Strongly Alters Organic Nitrogen Allocation in Maize and Stimulates Productivity of Systemic Source Leaves. *Plant Physiology*, 152(1), 293–308. <https://doi.org/10.1104/pp.109.147702>
- Hu, L., Mu, J., Su, P., Wu, H., Yu, G., Wang, G., Wang, L., Ma, X., Li, A., Wang, H., Zhao, L., & Kong, L. (2018). Multi-functional roles of TaSSI2 involved in Fusarium head blight and powdery mildew resistance and drought tolerance. *Journal of Integrative Agriculture*, 17(2), 368–380. [https://doi.org/10.1016/S2095-3119\(17\)61680-0](https://doi.org/10.1016/S2095-3119(17)61680-0)
- Huang, S., Van Aken, O., Schwarzländer, M., Belt, K., & Millar, A. H. (2016). The Roles of Mitochondrial Reactive Oxygen Species in Cellular Signaling and Stress Response in Plants. *Plant Physiology*, 171(3), 1551–1559. <https://doi.org/10.1104/pp.16.00166>
- Jin, M., Hu, S., Wu, Q., Feng, X., Zhang, Y., Jiang, Q., Ma, J., Qi, P., Chen, G., Jiang, Y., Zheng, Y., Wei, Y., & Xu, Q. (2024). An effector protein of Fusarium graminearum targets chloroplasts and suppresses cyclic photosynthetic electron flow. *Plant Physiology*, 196(4), 2422–2436. <https://doi.org/10.1093/plphys/kiae538>
- Kanehisa, M., & Goto, S. (2000). KEGG: Kyoto Encyclopedia of Genes and Genomes. *Nucleic Acids Research*, 28(1), 27–30. <https://doi.org/10.1093/nar/28.1.27>
- Kanehisa, M., Goto, S., Hattori, M., Aoki-Kinoshita, K. F., Itoh, M., Kawashima, S., Katayama, T., Araki, M., & Hirakawa, M. (2006). From genomics to chemical genomics: New developments in KEGG. *Nucleic Acids Research*, 34(suppl_1), D354–D357. <https://doi.org/10.1093/nar/gkj102>
- Kanehisa, M., Sato, Y., & Morishima, K. (2016). BlastKOALA and GhostKOALA: KEGG Tools for Functional Characterization of Genome and Metagenome Sequences. *Journal of Molecular Biology*, 428(4), 726–731. <https://doi.org/10.1016/j.jmb.2015.11.006>
- Kassambara, A. (2022). *rstatix: Pipe-Friendly Framework for Basic Statistical Tests*. (Version R Package Version 0.7.1) [Computer software]. <https://github.com/kassambara/rstatix>
- Kolde, R. (2019). *pheatmap: Pretty heatmaps* (Version R Package Version 1.0.12) [Computer software]. <https://github.com/raivokolde/pheatmap>
- Kretschmer, M., Damoo, D., Djamei, A., & Kronstad, J. (2020). Chloroplasts and Plant Immunity: Where Are the Fungal Effectors? *Pathogens*, 9(1), Article 1. <https://doi.org/10.3390/pathogens9010019>
- Lambert, I., Paysant-Le Roux, C., Colella, S., & Martin-Magniette, M.-L. (2020). DiCoExpress: A tool to process multifactorial RNAseq experiments from quality controls to co-expression analysis through differential analysis based on contrasts inside GLM models. *Plant Methods*, 16(1), 68. <https://doi.org/10.1186/s13007-020-00611-7>
- Lapin, D., & Van den Ackerveken, G. (2013). Susceptibility to plant disease: More than a failure of host immunity. *Trends in Plant Science*, 18(10), 546–554. <https://doi.org/10.1016/j.tplants.2013.05.005>
- Lee, W.-S., Fu, S.-F., Verchot-Lubicz, J., & Carr, J. P. (2011). Genetic modification of alternative respiration in *Nicotiana benthamiana* affects basal and salicylic acid-induced resistance to potato virus X. *BMC Plant Biology*, 11(1), 41. <https://doi.org/10.1186/1471-2229-11-41>
- Li, B., Hou, L., Song, C., Wang, Z., Xue, Q., Li, Y., Qin, J., Cao, N., Jia, C., Zhang, Y., & Shi, W. (2022). Biological function of calcium-sensing receptor (CAS) and its coupling calcium signaling in plants. *Plant Physiology and Biochemistry*, 180, 74–80. <https://doi.org/10.1016/j.plaphy.2022.03.032>
- Li, G., Zhou, J., Jia, H., Gao, Z., Fan, M., Luo, Y., Zhao, P., Xue, S., Li, N., Yuan, Y., Ma, S., Kong, Z., Jia, L., An, X., Jiang, G., Liu, W., Cao, W., Zhang, R., Fan, J., ... Ma, Z. (2019). Mutation of a histidine-rich calcium-binding-protein gene in wheat confers resistance to Fusarium head blight. *Nature Genetics*, 51(7), 1106–1112. <https://doi.org/10.1038/s41588-019-0426-7>
- Littlejohn, G. R., Breen, S., Smirnov, N., & Grant, M. (2021). Chloroplast immunity illuminated. *New Phytologist*, 229(6), 3088–3107. <https://doi.org/10.1111/nph.17076>
- Love, M. I., Huber, W., & Anders, S. (2014). Moderated estimation of fold change and dispersion for RNA-seq data with DESeq2. *Genome Biology*, 15(12), 550. <https://doi.org/10.1186/s13059-014-0550-8>
- Lu, Y., & Yao, J. (2018). Chloroplasts at the Crossroad of Photosynthesis, Pathogen Infection and Plant Defense. *International Journal of Molecular Sciences*, 19(12), Article 12. <https://doi.org/10.3390/ijms19123900>

- Ma, H.-X., Bai, G.-H., Gill, B. S., & Hart, L. P. (2006). Deletion of a Chromosome Arm Altered Wheat Resistance to Fusarium Head Blight and Deoxynivalenol Accumulation in Chinese Spring. *Plant Disease*, 90(12), 1545–1549. <https://doi.org/10.1094/PD-90-1545>
- Major, I. T., Nicole, M.-C., Duplessis, S., & Séguin, A. (2010). Photosynthetic and respiratory changes in leaves of poplar elicited by rust infection. *Photosynthesis Research*, 104(1), 41–48. <https://doi.org/10.1007/s11120-009-9507-2>
- McMullen, M., Bergstrom, G., De Wolf, E., Dill-Macky, R., Hershman, D., Shaner, G., & Van Sanford, D. (2012). A Unified Effort to Fight an Enemy of Wheat and Barley: Fusarium Head Blight. *Plant Disease*, 96(12), 1712–1728. <https://doi.org/10.1094/PDIS-03-12-0291-FE>
- Medina-Puche, L., Tan, H., Dogra, V., Wu, M., Rosas-Diaz, T., Wang, L., Ding, X., Zhang, D., Fu, X., Kim, C., & Lozano-Duran, R. (2020). A Defense Pathway Linking Plasma Membrane and Chloroplasts and Co-opted by Pathogens. *Cell*, 182(5), 1109–1124.e25. <https://doi.org/10.1016/j.cell.2020.07.020>
- Mesterhazy, A. (2020). Updating the Breeding Philosophy of Wheat to Fusarium Head Blight (FHB): Resistance Components, QTL Identification, and Phenotyping—A Review. *Plants*, 9(12), Article 12. <https://doi.org/10.3390/plants9121702>
- Murtagh, F., & Legendre, P. (2014). Ward's Hierarchical Agglomerative Clustering Method: Which Algorithms Implement Ward's Criterion? *Journal of Classification*, 31(3), 274–295. <https://doi.org/10.1007/s00357-014-9161-z>
- Nalam, V. J., Alam, S., Keereetaweep, J., Venables, B., Burdan, D., Lee, H., Trick, H. N., Sarowar, S., Makandar, R., & Shah, J. (2015). Facilitation of Fusarium graminearum Infection by 9-Lipoxygenases in Arabidopsis and Wheat. *Molecular Plant-Microbe Interactions*, 28(10), 1142–1152. <https://doi.org/10.1094/MPMI-04-15-0096-R>
- Osman, M., He, X., Singh, R. P., Duveiller, E., Lillemo, M., Pereyra, S. A., Westerdijk-Hoks, I., Kurushima, M., Yau, S.-K., Benedettelli, S., & Singh, P. K. (2015). Phenotypic and genotypic characterization of CIM-MYT's 15th international Fusarium head blight screening nursery of wheat. *Euphytica*, 205(2), 521–537. <https://doi.org/10.1007/s10681-015-1425-0>
- Parry, D. W., Jenkinson, P., & McLEOD, L. (1995). Fusarium ear blight (scab) in small grain cereals—A review. *Plant Pathology*, 44(2), 207–238. <https://doi.org/10.1111/j.1365-3059.1995.tb02773.x>
- Pavan, S., Jacobsen, E., Visser, R. G. F., & Bai, Y. (2010). Loss of susceptibility as a novel breeding strategy for durable and broad-spectrum resistance. *Molecular Breeding*, 25(1), 1–12. <https://doi.org/10.1007/s11032-009-9323-6>
- Plaxton, W. C., & Podestá, F. E. (2006). The Functional Organization and Control of Plant Respiration. *Critical Reviews in Plant Sciences*, 25(2), 159–198. <https://doi.org/10.1080/07352680600563876>
- R Core Team. (2021). R: a language and environment for statistical computing [Computer software]. Vienna: R Foundation for Statistical Computing.
- Robert, C., Bancal, M.-O., Lannou, C., & Ney, B. (2006). Quantification of the effects of Septoria tritici blotch on wheat leaf gas exchange with respect to lesion age, leaf number, and leaf nitrogen status. *Journal of Experimental Botany*, 57(1), 225–234. <https://doi.org/10.1093/jxb/eri153>
- Robinson, M. D., McCarthy, D. J., & Smyth, G. K. (2010). edgeR: A Bioconductor package for differential expression analysis of digital gene expression data. *Bioinformatics*, 26(1), 139–140. <https://doi.org/10.1093/bioinformatics/btp616>
- Rocher, F., Alouane, T., Philippe, G., Martin, M.-L., Label, P., Langin, T., & Bonhomme, L. (2022). Fusarium graminearum Infection Strategy in Wheat Involves a Highly Conserved Genetic Program That Controls the Expression of a Core Effectome. *International Journal of Molecular Sciences*, 23(3), Article 3. <https://doi.org/10.3390/ijms23031914>
- Rocher, F., Dou, S., Philippe, G., Martin, M.-L., Label, P., Langin, T., & Bonhomme, L. (2024). Integrative systems biology of wheat susceptibility to Fusarium graminearum uncovers a conserved gene regulatory network and identifies master regulators targeted by fungal core effectors. *BMC Biology*, 22(1), 53. <https://doi.org/10.1186/s12915-024-01852-x>
- Schneider, C. A., Rasband, W. S., & Eliceiri, K. W. (2012). NIH Image to ImageJ: 25 years of image analysis. *Nature Methods*, 9(7), 671–675. <https://doi.org/10.1038/nmeth.2089>
- Sørhagen, K., Laxa, M., Peterhänsel, C., & Reumann, S. (2013). The emerging role of photorespiration and non-photorespiratory peroxisomal metabolism in pathogen defence. *Plant Biology*, 15(4), 723–736. <https://doi.org/10.1111/j.1438-8677.2012.00723.x>
- Steiner, B., Buerstmayr, M., Michel, S., Schweiger, W., Lemmens, M., & Buerstmayr, H. (2017). Breeding strategies and advances in line selection for Fusarium head blight resistance in wheat. *Tropical Plant Pathology*, 42(3), 165–174. <https://doi.org/10.1007/s40858-017-0127-7>
- Su, P., Zhao, L., Li, W., Zhao, J., Yan, J., Ma, X., Li, A., Wang, H., & Kong, L. (2021). Integrated metabolo-transcriptomics and functional characterization reveals that the wheat auxin receptor TIR1 negatively regulates defense against Fusarium graminearum. *Journal of Integrative Plant Biology*, 63(2), 340–352. <https://doi.org/10.1111/jipb.12992>
- Su, Z., Bernardo, A., Tian, B., Chen, H., Wang, S., Ma, H., Cai, S., Liu, D., Zhang, D., Li, T., Trick, H., St. Amand, P., Yu, J., Zhang, Z., & Bai, G. (2019). A deletion mutation in TaHRC confers Fhb1 resistance to Fusarium head blight in wheat. *Nature Genetics*, 51(7), 1099–1105. <https://doi.org/10.1038/s41588-019-0425-8>
- Tatagiba, S. D., DaMatta, F. M., & Rodrigues, F. Á. (2015). Leaf Gas Exchange and Chlorophyll a Fluorescence Imaging of Rice Leaves Infected with Monographella albescens. *Phytopathology*, 105(2), 180–188. <https://doi.org/10.1094/PHYTO-04-14-0097-R>
- Tzelepis, G., Dörfors, F., Holmquist, L., & Dixelius, C. (2021). Plant mitochondria and chloroplasts are targeted by the Rhizoctonia solani RsCRP1 effector. *Biochemical and Biophysical Research Communications*, 544, 86–90. <https://doi.org/10.1016/j.bbrc.2021.01.019>
- van Dongen, J. T., Gupta, K. J., Ramírez-Aguilar, S. J., Araújo, W. L., Nunes-Nesi, A., & Fernie, A. R. (2011). Regulation of respiration in plants: A role for alternative metabolic pathways. *Journal of Plant Physiology*, 168(12), 1434–1443. <https://doi.org/10.1016/j.jplph.2010.11.004>
- van Schie, C. C. N., & Takken, F. L. W. (2014). Susceptibility Genes 101: How to Be a Good Host. *Annual Review of Phytopathology*, 52(Volume 52, 2014), 551–581. <https://doi.org/10.1146/annurev-phyto-102313-045854>
- Venske, E., dos Santos, R. S., Farias, D. da R., Rother, V., da Maia, L. C., Pegoraro, C., & Costa de Oliveira, A. (2019). Meta-Analysis of the QTLome of Fusarium Head Blight Resistance in Bread Wheat: Refining the Current Puzzle. *Frontiers in Plant Science*, 10. <https://doi.org/10.3389/fpls.2019.00727>
- Vogel, J. P., Raab, T. K., Schiff, C., & Somerville, S. C. (2002). PMR6, a Pectate Lyase-Like Gene Required for Powdery Mildew Susceptibility in Arabidopsis. *The Plant Cell*, 14(9), 2095–2106. <https://doi.org/10.1105/tpc.003509>
- Wang, J., Xu, G., Ning, Y., Wang, X., & Wang, G.-L. (2022). Mitochondrial functions in plant immunity. *Trends in Plant Science*, 27(10), 1063–1076. <https://doi.org/10.1016/j.tplants.2022.04.007>
- Xia, R., Schaafsma, A. W., Wu, F., & Hooker, D. C. (2020). Impact of the improvements in Fusarium head blight and agronomic management on economics of winter wheat. *World Mycotoxin Journal*, 13(3), 423–440. <https://doi.org/10.3920/WMJ2019.2518>
- Xu, G., Zhong, X., Shi, Y., Liu, Z., Jiang, N., Liu, J., Ding, B., Li, Z., Kang, H., Ning, Y., Liu, W., Guo, Z., Wang, G.-L., & Wang, X. (2020). A fungal effector targets a heat shock-dynamin protein complex to modulate mitochondrial dynamics and reduce plant immunity. *Science Advances*, 6(48), eabb7719. <https://doi.org/10.1126/sciadv.abb7719>
- Xu, Q., Tang, C., Wang, X., Sun, S., Zhao, J., Kang, Z., & Wang, X. (2019). An effector protein of the wheat stripe rust fungus targets

- chloroplasts and suppresses chloroplast function. *Nature Communications*, 10(1), 5571. <https://doi.org/10.1038/s41467-019-13487-6>
- Zaidi, S. S.-A., Mukhtar, M. S., & Mansoor, S. (2018). Genome Editing: Targeting Susceptibility Genes for Plant Disease Resistance. *Trends in Biotechnology*, 36(9), 898–906. <https://doi.org/10.1016/j.tibtech.2018.04.005>
- Zhang, Y., Yao, D., Yu, X., Cheng, X., Wen, L., Liu, C., Xu, Q., Deng, M., Jiang, Q., Qi, P., & Wei, Y. (2024). FgCWM1 modulates TaNDUFA9 to inhibit SA synthesis and reduce FHB resistance in wheat. *BMC Biology*, 22(1), 204. <https://doi.org/10.1186/s12915-024-02007-8>
- Zheng, T., Hua, C., Li, L., Sun, Z., Yuan, M., Bai, G., Humphreys, G., & Li, T. (2021). Integration of meta-QTL discovery with omics: Towards a molecular breeding platform for improving wheat resistance to Fusarium head blight. *The Crop Journal*, 9(4), 739–749. <https://doi.org/10.1016/j.cj.2020.10.006>

SUPPORTING INFORMATION

Additional supporting information can be found online in the Supporting Information section at the end of this article.

How to cite this article: Rocher, F., Bancal, P., Fortineau, A., Philippe, G., Label, P., Langin, T. et al. (2025) Unravelling ecophysiological and molecular adjustments in the photosynthesis-respiration balance during *Fusarium graminearum* infection in wheat spikes. *Physiologia Plantarum*, 177(2), e70150. Available from: <https://doi.org/10.1111/ppl.70150>